Atmospheric Environment 247 (2021) 118063

Contents lists available at ScienceDirect

Atmospheric Environment

journal homepage: http://www.elsevier.com/locate/atmosenv

Modelling air quality during the EXPLORE-YRD campaign – Part II. Regional source apportionment of ozone and $PM_{2.5}$

Lin Li [a], Jianlin Hu [a,*], Jingyi Li [a], Kangjia Gong [a], Xueying Wang [a], Qi Ying [b], Momei Qin [a], Hong Liao [a], Song Guo [c], Min Hu [c], Yuanhang Zhang [c,d]

[a] Jiangsu Key Laboratory of Atmospheric Environment Monitoring and Pollution Control, Collaborative Innovation Center of Atmospheric Environment and Equipment Technology, Nanjing University of Information Science & Technology, Nanjing, 210044, China
[b] Zachry Department of Civil Engineering, Texas A&M University, College Station, TX, 77843, USA
[c] State Key Joint Laboratory of Environmental Simulation and Pollution Control, College of Environmental Sciences and Engineering, Peking University, Beijing, 100871, China
[d] CAS Center for Excellence in Regional Atmospheric Environment, Chinese Academy of Science, Xiamen, 361021, China

HIGHLIGHTS

- Regional source apportionment is conducted for O3 and PM2.5 during the EXPLORE-YRD campaign.
- Anthropogenic sources dominate the formation of O3 and PM2.5 pollution in YRD.
- Industry and transportation are generally the two largest sources of O3 and PM2.5 in YRD.
- Reducing emissions from industry and transportation should be considered for simultaneous control of O3 and PM2.5 in YRD.

ARTICLE INFO

Keywords:
Source apportionment
Ozone
$PM_{2.5}$
Yangtze river delta region
EXPLORE-YRD

ABSTRACT

A source-oriented Community Multiscale Air Quality model was used to quantify the contributions of different sources to ground-level fine particulate matter ($PM_{2.5}$) and ozone (O_3) over the Yangtze River Delta (YRD) region during the EXPLORE-YRD (EXPeriment on the eLucidation of the atmospheric Oxidation capacity and aerosol foRmation, and their Effects in the Yangtze River Delta) campaign (17 May to June 17, 2018). O_3 formation in most urban areas of YRD is attributed to volatile organic compounds (VOCs) (81.1%, 78.5%, 60.2%, and 55.1% in Shanghai, Nanjing, Hefei, and Hangzhou, respectively), but is affected more by nitrogen oxides (NOx) in suburban and rural areas. Industry and transportation are the two major sources of O_3 and $PM_{2.5}$. In addition to the two sources, NOx produced owing to power generation, and VOC emissions from biogenic sources are important source of O_3. Industry contributes the most to the total mass of $PM_{2.5}$ in the YRD during the study period (9–25 $\mu g/m^3$), followed by transportation (2–7 $\mu g/m^3$). Industry, residential emissions, and transportation are the major sources of primary organic carbon and elemental carbon, whereas industry, transportation, and power generation account for most of the sulphate ($SO2-$ 4) and nitrate ($NO-$ 3) in the YRD. Agriculture is the most dominant source of ammonium emissions ($NH+$ 4). In Shanghai, Nanjing, Hefei, and Taizhou, secondary organic aerosol (SOA) are mainly contributed by industrial emissions. However, in Hangzhou, biogenic emissions contribute more than 40% of SOA. During all types of pollution episodes, industry and transportation are generally the two greatest sources of O_3 and $PM_{2.5}$ in YRD. The contribution of industry is higher during high $PM_{2.5}$ pollution episodes, whereas biogenic and open burning contributions are more important during high O_3 episodes. Overall, anthropogenic sources dominate the formation of O_3 and $PM_{2.5}$ pollution in the YRD, whereas biogenic emissions contribute significantly to O_3 attributable to VOC emissions (O_3_VOCs) accounting for 9–20% in urban areas of the YRD.

* Corresponding author.
E-mail address: jianlinhu@nuist.edu.cn (J. Hu).

https://doi.org/10.1016/j.atmosenv.2020.118063
Received 14 May 2020; Received in revised form 31 October 2020; Accepted 4 November 2020
Available online 5 January 2021

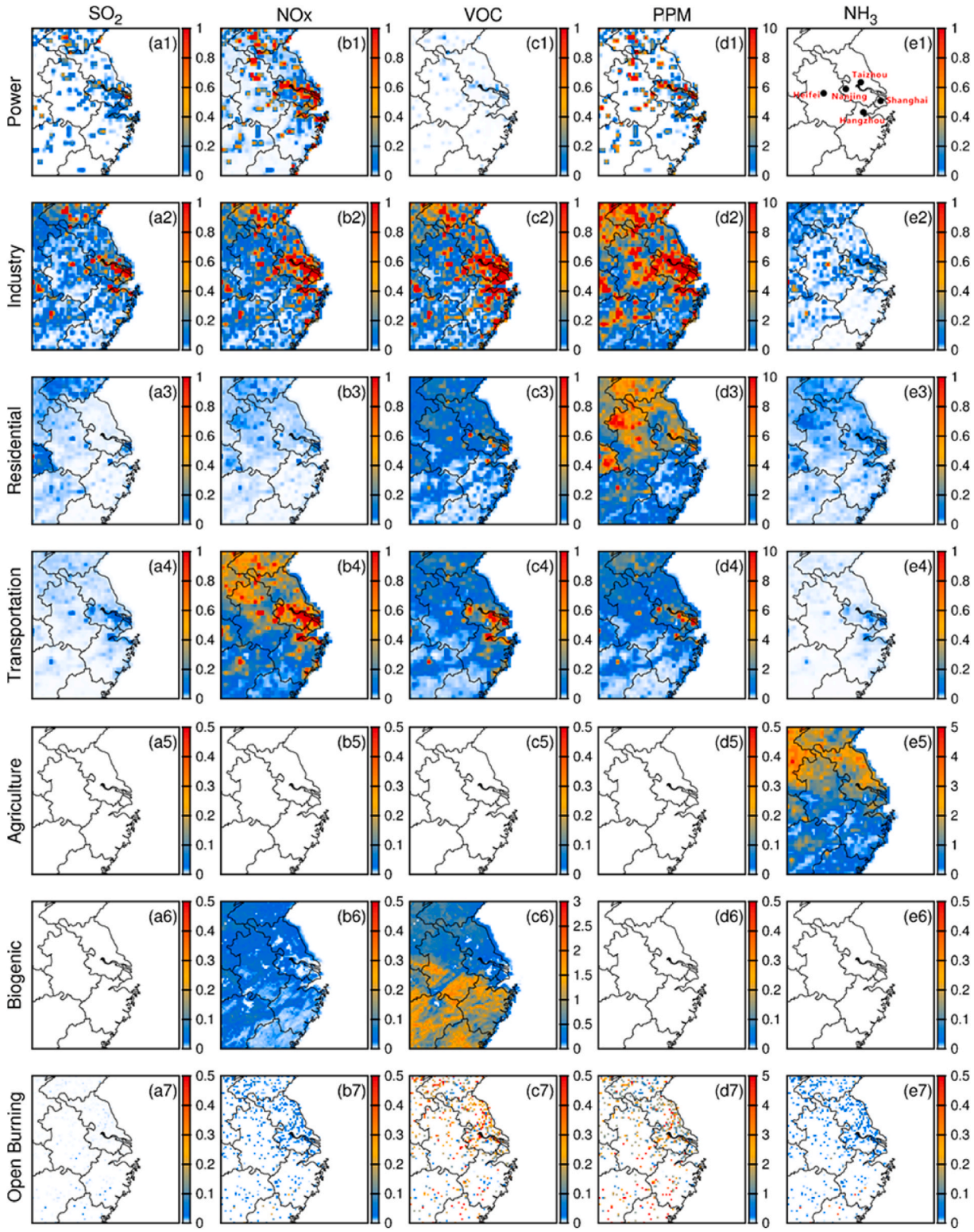

Fig. 1. Spatial distribution of the emission rates of SO_2, NOx, VOC, PPM and NH_3 from different source categories over the YRD region. Units are molecules/s for SO_2, NOx, VOC, NH_3, and g/s for PPM. Black dots in panel (e1) mark geographical positions of Nanjing, Taizhou, Hefei, Shanghai and Hangzhou, respectively.

1. Introduction

Since an extreme haze pollution event in 2013, air pollution has become a major public concern in China. Particulate matter with an aerodynamic diameter less than or equal to 2.5 μm ($PM_{2.5}$) is the dominant pollutant that causes haze pollution. $PM_{2.5}$ is harmful to human health and has severe effects on ecosystems and climate (Hu et al., 2017; Lall et al., 2004; Menon et al., 2008; Qiao et al., 2015). In China, in the past few years, strict emission control measures have been employed and $PM_{2.5}$ levels have been greatly reduced (Fan et al., 2020; Wang et al., 2016; Zhang et al., 2015). However, $PM_{2.5}$ levels in most cities are still high, with annual average concentrations exceeding the

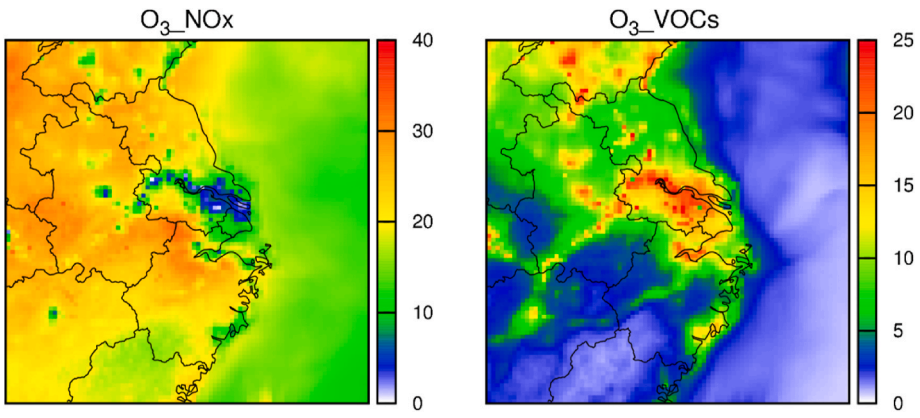

Fig. 2. Average MDA8 O_3 concentrations attributed to NOx and VOCs. Units are ppb.

Table 1
Contributions of NOx and VOCs to MDA8 O_3 concentrations in different cities.

	NJ	TZ	HF	SH	HZ
NOx	21.5%	52.2%	39.8%	18.9%	44.9%
VOCs	78.5%	47.8%	60.2%	81.1%	55.1%

Chinese Ambient Air Quality Standards of 35 μg/m^3. Contrary to the rapid decrease in $PM_{2.5}$, ozone (O_3), a major component of photochemical smog pollution, has been increasing over the last few years (Gao et al., 2017; Ma et al., 2016; Ou et al., 2016; Wang et al., 2017). Exposure to high O_3 concentrations also adversely affects human health and ecosystems (Feng et al., 2014; Liu et al., 2013). With the worsening O_3 pollution trend, O_3 has gradually become another pollutant of concern in China. Pollution controls are urgently needed to further reduce $PM_{2.5}$ pollution and to solve the worsening O_3 pollution.

The Yangtze River Delta (YRD) region, including the Shanghai municipality, and Jiangsu, Zhejiang, and Anhui provinces, is one of the fastest developing economic zones in China. The YRD region suffers from both $PM_{2.5}$ and O_3 pollution problems driven by rapid economic development, industrialisation, and urbanisation. To better understand the formation and sources of O_3 and $PM_{2.5}$ in the YRD region, a comprehensive campaign study, EXPeriment on the eLucidation of the atmospheric Oxidation capacity and aerosol foRmation, and their Effects in the Yangtze River Delta (EXPLORE-YRD), was conducted at a regional site of Taizhou from 17 May to June 17, 2018. Identifying and quantifying the emission sources that contribute to $PM_{2.5}$ and O_3 are essential for developing efficient emission control measures to improve air quality in YRD.

Previous studies have investigated the contributions of various emission sources to $PM_{2.5}$ and its major components in different regions of China (Hu et al., 2015; Li et al., 2017; Liu et al., 2016; Qiao et al., 2018; Timmermans et al., 2017; Wang et al., 2015). A few $PM_{2.5}$ source apportionment studies have also been conducted in the YRD region. For example, Li et al. (2015) found that industrial processing (12.7–38.7%), combustion emissions (21.7–37.3%), mobile source emissions (7.5–17.7%), and fugitive dust (8.4–27.3%) were the four major source categories contributing to the high haze pollution in the YRD region. Hua et al. (2015) pointed out that vehicle emissions and biomass burning were the most important primary sources of $PM_{2.5}$ in the YRD region. A few studies have also investigated the sources of O_3 in the YRD region. Li et al. (2016) and Li et al. (2019) adopted the Comprehensive Air Quality Model with Extensions with O_3 source apportionment technology to investigate the contribution of different regions and source categories to surface O_3 in the YRD region during 2013 and 2015, respectively. Both studies showed that industries and vehicles were the two most important emission sources contributing to O_3.

Currently, the YRD region faces both $PM_{2.5}$ and O_3 pollution and requires the use of emissions control strategies to reduce the two pollutants. Because previous source apportionment studies focused on either $PM_{2.5}$ or O_3, they could not provide information on whether there are common sources of $PM_{2.5}$ and O_3 in this region. To answer this question, this study quantifies the contributions of different sources to $PM_{2.5}$ and O_3 in the YRD region during the EXPLORE-YRD campaign. A source-oriented chemical transport model was applied to track $PM_{2.5}$ and O_3 contributed by precursors from different sources during atmospheric chemical and physical processes. Source contributions to non-background O_3 (including O_3 attributed to nitrogen oxides (NOx) (O_3_NOx) and O_3 attributed to volatile organic compounds (VOCs) (O_3_VOCs)) were estimated. The contributions of different sources to the total $PM_{2.5}$ mass and the major components of $PM_{2.5}$ (primary $PM_{2.5}$ (PPM), secondary inorganic $PM_{2.5}$ (i.e., sulphate (SO2− 4), nitrate (NO−

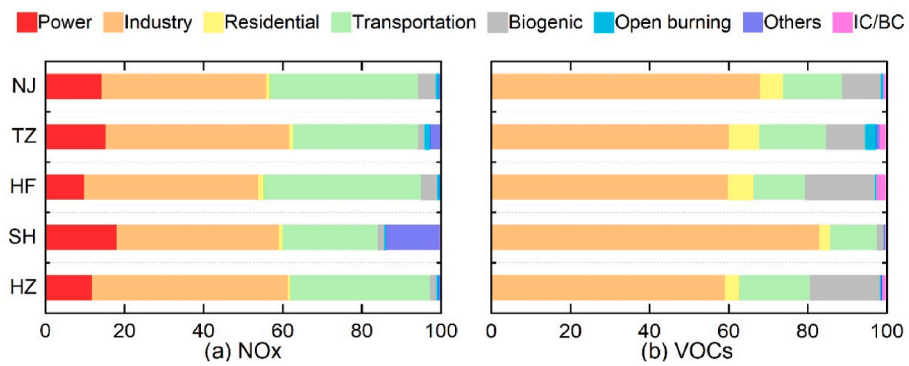

Fig. 3. The percentage source contributions of MDA8 O_3 from (a) NOx and (b) VOCs in different cities. "Others" means contributions due to emissions from other countries. IC/BC is the contributions of O_3 produced due to NOx and VOCs entered the domain through initial and boundary conditions.

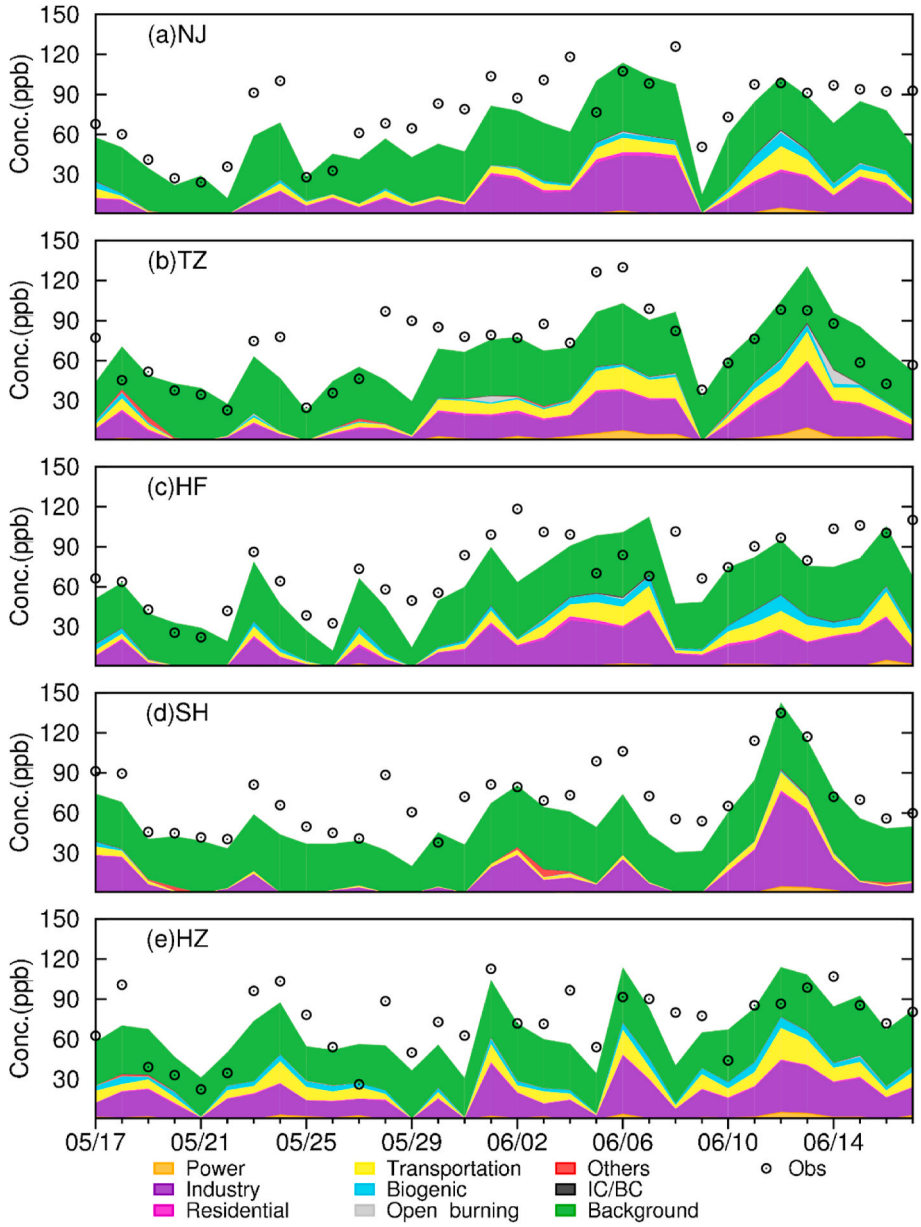

Fig. 4. Daily source contributions to total MDA8 O_3 at five study sites. Observed O_3 concentrations are marked by the circles, and simulated O_3 concentrations from different sources are indicated by the colored areas. O_3 directly entering the domain through initial and boundary conditions are regarded as background O_3.

3), ammonium (NH_4^+), and secondary organic aerosols (SOA) were also quantified. The results provide insights for designing practical control strategies to simultaneously mitigate $PM_{2.5}$ and O_3 pollution in the YRD region.

2. Methodology

2.1. Model description

The source-oriented Community Multiscale Air Quality (CMAQ) model has been developed and updated in numerous previous studies (Ying et al., 2018; Zhang et al., 2014; Zhang and Ying, 2011a, b). In this study, the source apportionment methods for different pollutants were merged into one framework to simultaneously calculate the source contributions to O_3 and $PM_{2.5}$. Here, we briefly summarise the methods used to determine the source contributions to O_3 and $PM_{2.5}$ in the model.

The contributions of different emission sources to O_3 were determined using an improved O_3 source apportionment method, as described by Wang et al. (2019b). This method considers O_3_NOx and O_3_VOCs in three O_3 sensitivity regimes, that is, NOx-limited, VOC-limited, and transition regimes. A detailed description of the regime classification is provided by Wang et al. (2019a). After the amount of O_3_NOx and O_3_VOCs is determined in each time step, contributions from different sources to NOx and VOCs are apportioned using reactive source-tagged tracers. An expanded photochemical mechanism (SAPRC11 in this study) was used in the source-oriented framework to track NOx, primary VOCs, and their reaction products from different sources. This method has been applied previously to quantify the contributions of different sources to summertime O_3 in China in August 2013 (Wang et al., 2019b), and more details can be found in the paper and the references therein.

Source apportionment of $PM_{2.5}$ was achieved by tracking the contributions of different sources to PPM, SO_4^{2-}, NO_3^-, NH_4^+, and SOA. Source contributions to PPM were determined using non-reactive PPM tracers, which represent a small fraction (0.001%) of the total PPM mass emitted from given sources and have no obvious effects on the particle

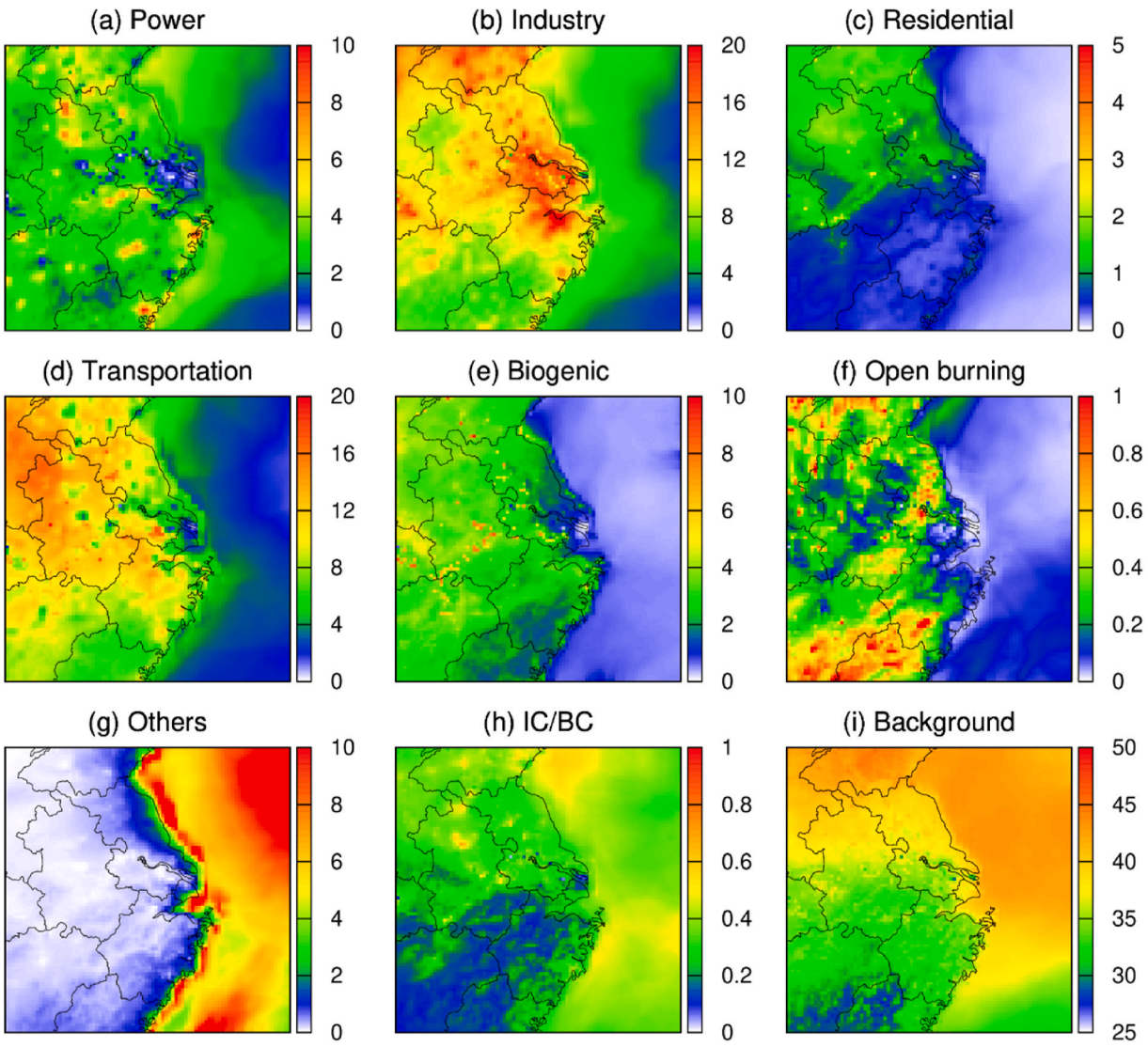

Fig. 5. Average MDA8 O_3 concentrations attributed to (a) power, (b) industry, (c) residential, (d) transportation, (e) biogenic, (f) open burning, (g) others, (h) IC/BC and (i) background. Units are ppb.

mass and size distribution. Hu et al. (2015) and Shi et al. (2017) applied this method to the CMAQ to evaluate the source contributions of important primary $PM_{2.5}$ components (such as primary organic carbon (POC) and elemental carbon (EC)) in China. More detailed descriptions of this method can be found in the above references.

SO2− 4, NO− 3, and NH+ 4 were identified as the dominant contributors to the $PM_{2.5}$ mass in China, accounting for 40–60% (Wu et al., 2015; Yang et al., 2011). NOx, SO_2, and NH_3 emissions from different sources and their chemical reaction products were tagged to track the source contributions to NO− 3, SO2− 4, and NH+ 4, respectively. The chemical mechanism is largely expanded to accommodate these changes in the source-oriented framework. Shi et al. (2017) explained this apportionment method and applied it to quantify the source contributions to NO− 3, SO2− 4, and NH+ 4 in China in 2013.

The source apportionment of SOA was modified based on the method described by Wang et al. (2018) and Liu et al. (2020). Using the method of Wang et al. (2018), only one source can be tracked in a single simulation; therefore, multiple simulations need to be conducted to obtain the contributions of all sources. In this study, this approach was improved to track nine sources simultaneously in the model.

After determining the contributions of different sources to PPM, NO− 3, SO2− 4, NH+ 4, and SOA, the source contributions to the total $PM_{2.5}$ mass can be quantified.

2.2. Model application

The CMAQ model version 5.0.2 was applied in our base case study to simulate the air quality in the YRD region during the EXPLORE_YRD campaign (Wang et al., 2020). Details about the model updates and configurations as well as the input data for the meteorological, emissions, and initial/boundary conditions are described in the base case study (Wang et al., 2020). We conducted a source-oriented CMAQ model simulation in the YRD region for the entire period of the EXPLORE-YRD campaign from 14 May to June 17, 2018. The first 3 days were used as spin-up to reduce the effect of initial conditions and are not included in the analyses. The base case study indicated that the air quality predictions, especially for $PM_{2.5}$, were relatively more accurate with the meteorological fields generated using the ECMWF Reanalysis v5 (ERA5) data to drive the Weather Research and Forecasting model. Therefore, ERA5 meteorological fields were used in this study to simultaneously track the sources of $PM_{2.5}$ and O_3 with the expanded photochemical mechanism. A horizontal resolution of 12 km was used in this study because the base case study showed that the difference in accuracy using resolutions of 12 and 4 km was small, while the computational efficiency

Table 2
Comparison of results in previous MDA8 O_3 source apportionment studies in YRD and in present study.

References	Method	Study period	Main source(s)	Contribution (s)
Li et al. (2016)	CAMx (OSAT)	July 2013	Industry[a]	24.5%–34%
			Transportation[b]	11%–15.5%
			Power	3.5%–6.5%
			Residential	~0.3%
			Biogenic	18.5%–25%
Wang et al. (2019b)	CMAQ	August 2013	Industry	27%–47%
			Transportation	11%–24%
			Power	11%–17%
			Residential	~2.5%
			Biogenic	18.5%–26.5%
Li et al. (2019)	CAMx (OSAT)	August 2015	Transportation[c]	35%–51%
			Industry	11.9%–23.5%
			Combustion[d]	16%–23%
			Residential	3%–5%
			Biogenic	9.5%–20%
Shu et al. (2020)	CAMx (OSAT)	2013–2017	Transportation	22.2%–29.8%
			Industry	25.1%–25.9%
			Power	10%–25%
			Residential	0.8–1.3%
			Biogenic	5.9%–9.5%
This study	CMAQ	17 May to June 17, 2018	Industry	52%–75%
			Transportation	13%–25%
			Power	3.4%–8.3%
			Residential	2.3%–5%
			Biogenic	1.1%–8.8%

Industry[a] is total of industrial boiler and kilns and industrial process in the paper; Transportation[b] refers mobile source in the paper; Transportation[c] is mobile source in the paper; Combustion[d] is total of powerplant and boiler in the paper.

using a resolution of 12 km was much higher.

Contributions from eight emission sources to $PM_{2.5}$ and O_3 were tracked in this study, including power generation, industry, residential, transportation, agriculture, biogenic emissions, open burning, and emissions in other countries. The Multi-resolution Emission Inventory for China of the year 2016 (http://www.meicmodel.org/) was grouped into five sectors (i.e., power, industry, residential, transportation, and agriculture). In addition, the Regional Emission inventory in ASia version 2 provided emissions from other countries and regions outside China. Open burning emissions data were collected from the Fire INventory from NCAR, which is a daily fire emissions product for atmospheric chemistry models. The global Model of Emissions of Gases and Aerosols from Nature version 2.1 was used to evaluate biogenic emissions. More details about the emission processing can be found in the study of Hu et al. (2015).

Fig. 1 shows the emissions of SO_2, NOx, VOCs, PPM, and NH_3 from different source categories in the YRD region during the study period. The power sector mainly emits NOx and PPM along the Yangtze River in Jiangsu Province and in several areas in Shandong and Anhui provinces. Among the seven sectors, the industrial sector is a major contributor to SO_2, NOx, VOCs, and PPM with similar spatial distributions. The greatest NOx emissions are from transportation mostly located in Shanghai, south Jiangsu Province, and north Anhui Province. The high emissions of PPM attributed to residential areas should not be ignored. Agriculture is the largest contributor to NH_3 emissions, which are mainly concentrated in the north and east Jiangsu Province and the part of Henan Province in the study area. The contribution of biogenic sources to VOCs is clearly higher than that of NOx. Compared to other emitted species, open burning is an important contributor to PPM.

3. Results and discussion

3.1. Source apportionment of O_3

3.1.1. O_3 formation attributed to NOx and VOCs in the YRD

Fig. 2 shows the spatial distribution of non-background maximum daily 8-h average (MDA8) O_3 attributed to NOx and VOCs during the EXPLORE-YRD campaign period over the YRD region. Low NOx and high VOCs contributions are found in the core areas of the YRD, that is, Shanghai, southern Jiangsu Province, Hangzhou Bay area, and Hefei, suggesting that O_3 is mainly VOC-limited in these areas. The contribution of NOx is higher than that of VOCs in other areas of the YRD. Table 1 summarises the fractional contributions of averaged MDA8 O_3 contributed by NOx and VOCs in Nanjing (NJ), Taizhou (TZ), Hefei (HF), Shanghai (SH), and Hangzhou (HZ) cities. VOC sources play a more important role than NOx, and contribute to 81.1%, 78.5%, 60.2%, and 55.1% of total O_3 produced in SH (14.5 ppb), NJ (21.2 ppb), HF (17.1 ppb), and HZ (18.4 ppb), respectively. This result is consistent with previous studies that show that O_3 in the YRD region is VOC-limited in major urban areas (An et al., 2015; Geng et al., 2007, 2008). The contribution of O_3_NOx in TZ (52.2%) is slightly higher than that of O_3_VOCs (47.8%); therefore, NOx and VOCs are almost equally important for O_3 formation in TZ.

Fig. 3 displays the source proportions of MDA8 O_3 from NOx and VOCs in the five cities. IC/BC is classified as O_3 contributed by NOx and VOCs through initial and boundary conditions. As the contribution of agriculture is zero, its contribution is not calculated (corresponding to no NOx and VOC emissions, as shown in Fig. 1). Industry, transportation, and power generation are the top three source sectors contributing to O_3_NOx, with fractions of 41–50%, 24–40%, and 9–19%, respectively. Pollution from other countries is an important contributor (accounting for 13.7%) to O_3_NOx in SH during the campaign period. Industry, transportation, biogenic sources, and residential sectors are the four greatest sources of O_3_VOCs. The contributions from industry account for over 60% of the total O_3_VOCs in the five cities, with the largest proportion in SH (approximately 83%). The contribution of transportation to O_3_VOCs is 17.9%, 16.9%, 15%, 13%, and 11.9% in HZ, TZ, NJ, HF, and SH, respectively. Biogenic emissions contribute slightly to O_3_NOx but contribute 17.9%, 17.7%, 10%, and 9.7% to O_3_VOCs in HZ, HF, TZ, and NJ, respectively.

3.1.2. Regional source apportionment of O_3 in the YRD

Fig. 4 shows the time series of the predicted and measured MDA8 O_3 concentrations in the five cities. Total O_3 comprises O_3 produced by photochemistry and background O_3 (O_3 directly entering the domain through initial and boundary conditions is regarded as background O_3) in the model. The predicted total O_3 mixing ratios are in good agreement with the observed values and temporal variations. Background O_3 is relatively stable and accounts for more than half of the total O_3 when its total concentration is relatively low, especially at the end of May and the beginning of June in SH. Not considering the background O_3, industry is a vital emission sector that leads to O_3 pollution in the YRD region, with a maximum contribution reaching ~18 ppb during the study period. In addition, transportation contributes significantly in urban locations. The non-background O_3 produced as a result of NOx and VOC emissions has a substantial contribution to high O_3 days. The results demonstrate that high O_3 levels mainly result from the joint efforts of industry and transportation in the urban areas of the YRD region.

Fig. 5 shows the different source contributions to O_3 over the YRD region. The background O_3 has an even spatial distribution, with concentrations gradually increasing from 30 to 35 ppb in south YRD to approximately 40 ppb in north YRD. For non-background O_3, industry and transportation, the two dominant sources contributing to O_3, have different spatial distributions. The contribution of industry (~22 ppb) is mainly in Shanghai, the southern Jiangsu Province, and the northern Zhejiang Province. However, high O_3 concentrations, with a maximum

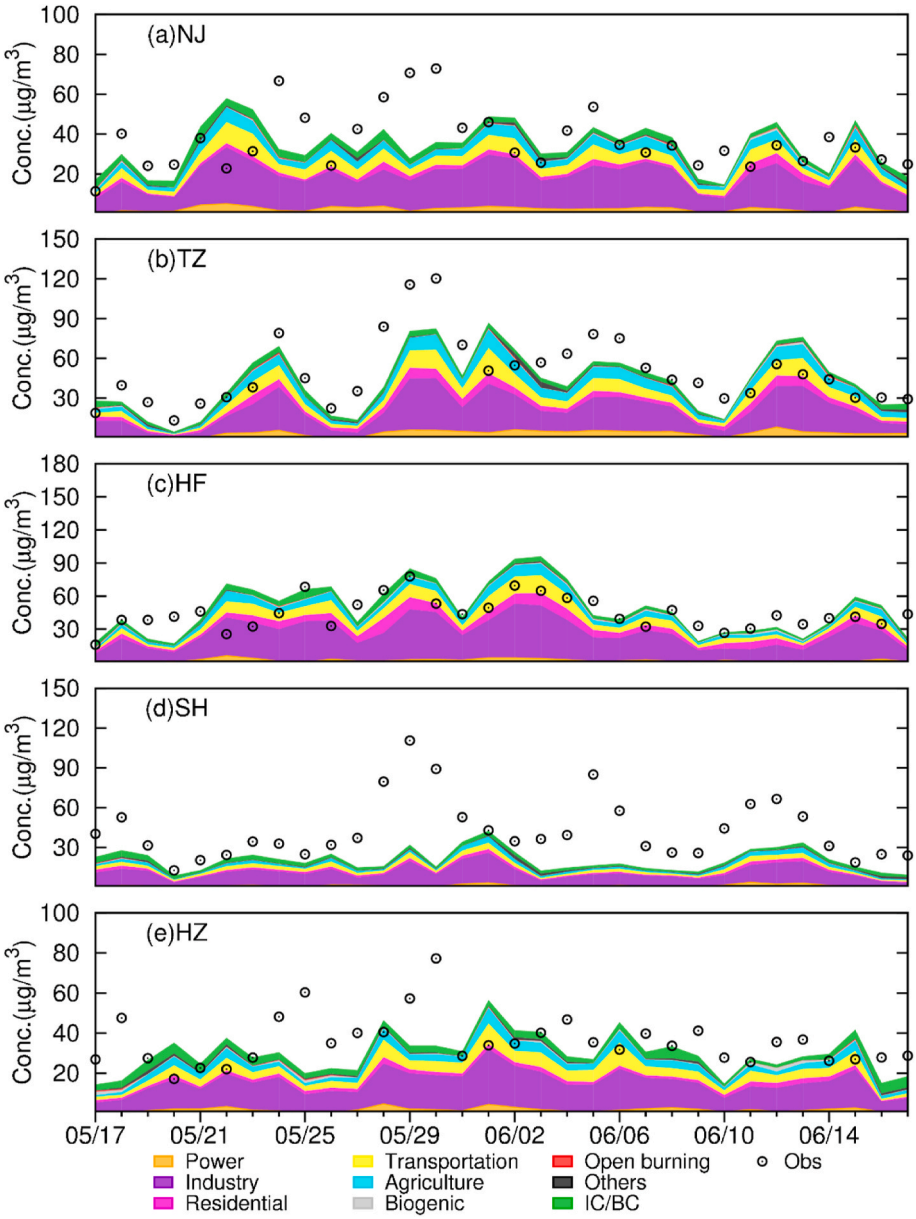

Fig. 6. Daily source contributions to average $PM_{2.5}$ at five urban sites. Observed $PM_{2.5}$ concentrations are marked by the circles, and simulated $PM_{2.5}$ concentrations from different sources are indicated by the colored areas.

of 16 ppb attributed to transportation, are located in the northwest part of the YRD region. The contribution of power generation to O_3 is scattered in space, with high contributions of up to 10 ppb in a few areas where power plants are located. The contribution of biogenic sources is approximately 2–4 ppb in most YRD regions during the study period, with relatively lower contributions along the coast. Residential source contribution reaches over 2 ppb in the north of Anhui and Jiangsu provinces and is less than 1 ppb in other YRD areas such as Zhejiang Province. In general, the contribution of open burning, IC/BC, and emissions from outside China are small for inland areas in the YRD, although emissions outside China can contribute up to 10 ppb over the East China Ocean and a few ppb for areas near the coast.

Table 2 compares the O_3 source apportionment results of this study with the results of a few previous studies conducted in the YRD region. Despite the different time periods and different methods used in different studies, industry and transportation were identified as the top two anthropogenic emission sources contributing to O_3 in most studies. The proportion of O_3 concentration contributed by transportation in this study is comparable to that reported by Wang et al. (2019b), but the contribution of industry is greater than that in previous studies. This discrepancy is likely due to the different time periods and emission inventories applied. In addition, in the emission inventory used in the current study, commercial solvent usage is included in the industry sector, which may have enhanced the contribution of industry. The contribution of biogenic sources to O_3 is lower than that in previous studies as biogenic emissions in May and June are lower than those in July and August.

3.2. Source apportionment of $PM_{2.5}$

3.2.1. Regional source apportionment of total mass of $PM_{2.5}$

Fig. 6 shows the time series of the source contributions of different sources to 24-h average $PM_{2.5}$ concentrations in the five cities. The observed $PM_{2.5}$ concentrations are also illustrated in the figure. The predicted total values of $PM_{2.5}$, which are the sum of the contributions of all sources, capture the observed concentrations and variations in most

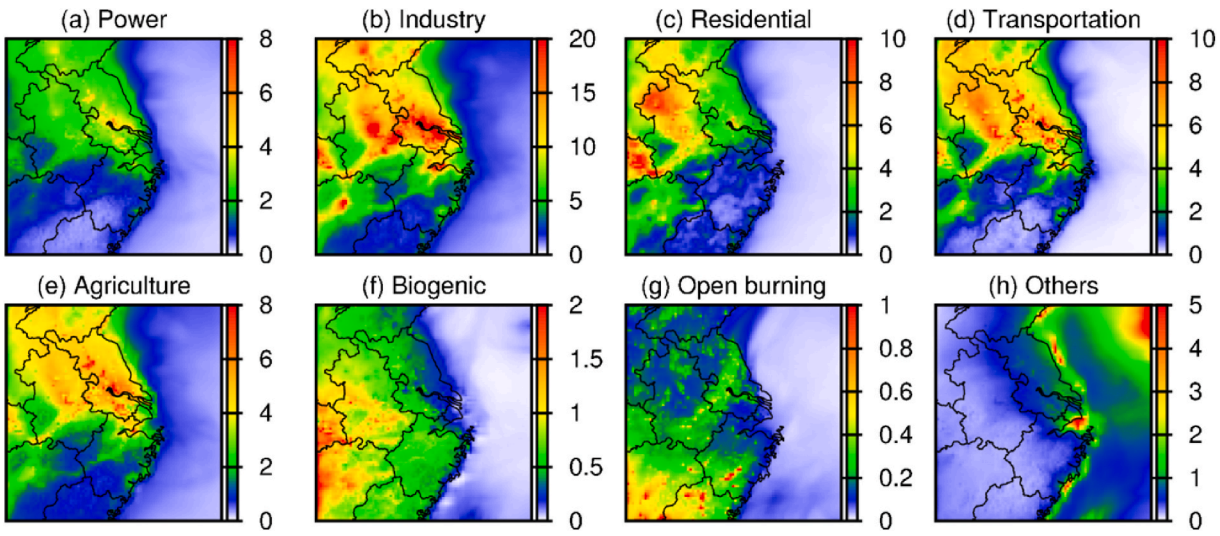

Fig. 7. Average 24-h $PM_{2.5}$ concentrations attributed to (a) power, (b) industry, (c) residential, (d) transportation, (f) biogenic, (g) open burning and (h) others. Units are $\mu g/m^3$.

Table 3
Comparison of results of previous $PM_{2.5}$ source apportionment studies in YRD and in present study.

References	Method	Study period	Main source(s)	Contribution (s)
Hua et al. (2015)	CMB	10 to November 15, 2011	Transportation[a]	6%–22%
			Biomass burning[b]	16%–26%
			Industry[c]	7%–12%
			Residential[d]	~5%
Timmermans et al. (2017)	LOTOS-EUROS	2013	Industry	34.4%
			Residential[e]	21.4%
			Transportation	19.9%
			Power	10.7%
			Agriculture	7.2%
Shi et al. (2017)	CMAQ	2013	Industry	28%–40%
			Residential	12%–24%
			Agriculture	12%–13%
			Power	11%–13%
			Transportation	6%–7%
			Open burning	~0.07%
Li et al. (2015)	CAMx (PSAT)	January 2013	Combustion[f]	21.7%–37.3%
			Industry[g]	12.7–38.7%
			Transportation[h]	7.5–17.7%
			Agriculture	2.5%–9.2%
			Biogenic	~0.05%
Qiao et al. (2018)	CMAQ	2013	Industry	37%–40%
			Residential	10.7%–19%
			Power	11.7%–13.5%
			Agriculture	9.4%–12%
			Transportation	6.6%–9.1%
			Open burning	1.8%–2.5%
This study	CMAQ	17 May to June 17, 2018	Industry	40%–50%
			Transportation	11.5%–16.2%
			Agriculture	9%–14.2%
			Residential	5.9%–12.2%
			Power	4.5%–9%
			Open burning	~0.5%
			Biogenic	~1.8%

Transportation[a] refers to vehicle in the study; Biomass burning[b] is total of residential biomass burning and open burning; Industry[c] is total of industrial coal and steel manufacture; Residential[d] refers to residential gas in the study; Residential[e] is residential combustion in the study; Combustion[f] considers coal and oil combustion from industrial boilers, kilns, power plants; Industry[g] is industrial processing; Transportation[h] is mobile source in the study.

cities, although the model underestimates $PM_{2.5}$ in SH and does not predict the high $PM_{2.5}$ pollution at the end of May. Compared to the contributions of IC/BC to O_3, the contributions of IC/BC to $PM_{2.5}$ should not be ignored (12.0%, 11.1%, 8.7%, 7.3%, and 7.1% in SH, HZ, NJ, HF, and TZ, respectively). Without considering the contributions of IC/BC, the industrial sector is the largest source contributing to $PM_{2.5}$ total mass (9–25 $\mu g/m^3$) during the study period, followed by transportation (2–7 $\mu g/m^3$) and agriculture (~6.5 $\mu g/m^3$). The residential sector contributes to $PM_{2.5}$ by 13.2%, 10.5%, 8.7%, 6.6%, and 6.6% in HF, TZ, SH, NJ, and HZ, respectively. Power generation contributes up to 9.7%, 9.0%, 8.7%, 7.8%, and 5.1% in TZ, NJ, SH, HZ, and HF, respectively. The contribution of biogenic emissions to $PM_{2.5}$ total mass is relatively low.

Fig. 7 presents the spatial distribution of different source contributions to the average $PM_{2.5}$ total mass concentrations during the campaign period. High contributions from industry (maximum of ~30 $\mu g/m^3$) and transportation (~9 $\mu g/m^3$) are located in the core YRD areas (Shanghai, southern Jiangsu Province, and Hangzhou Bay) and central Anhui Province. $PM_{2.5}$ contributed by residential emissions are mainly important in the northern Anhui Province with concentrations of up to 10 $\mu g/m^3$. Agriculture also contributes 5–8 $\mu g/m^3$ in most areas in Jiangsu and Anhui provinces. Power generation, industry, residential, transportation, and agriculture have lower contributions in the southeast regions.

Table 3 compares the $PM_{2.5}$ source apportionment results in the YRD reported in previous studies and in the present study. Industry is the most important source of $PM_{2.5}$ in the YRD in most studies, except in the study of Hua et al. (2015), which used the chemical mass balance method and only considered the primary $PM_{2.5}$. Residential emissions were the second largest $PM_{2.5}$ source in the YRD in numerous studies (Qiao et al., 2018; Shi et al., 2017; Timmermans et al., 2017) because these studies focused on a full-year or high $PM_{2.5}$ concentration days, which were mostly in winter when residential emissions became much higher. In the May–June episode investigated in this study, the contribution of residential emissions is lower. The contributions of other sources, such as power generation, agriculture, and transportation, are similar.

3.2.2. *Source contribution to $PM_{2.5}$ components*

Fig. 8 shows the average source contributions to $PM_{2.5}$ components (EC, POC, SO_4^{2-}, NO_3^-, NH_4^+, and SOA) in NJ, TZ, HF, SH, and HZ during the study period. EC concentrations in the five cities range from 1.78 $\mu g/m^3$ in SH to 3.65 $\mu g/m^3$ in HF. Industry, transportation, and residential emissions are the three major source sectors contributing to

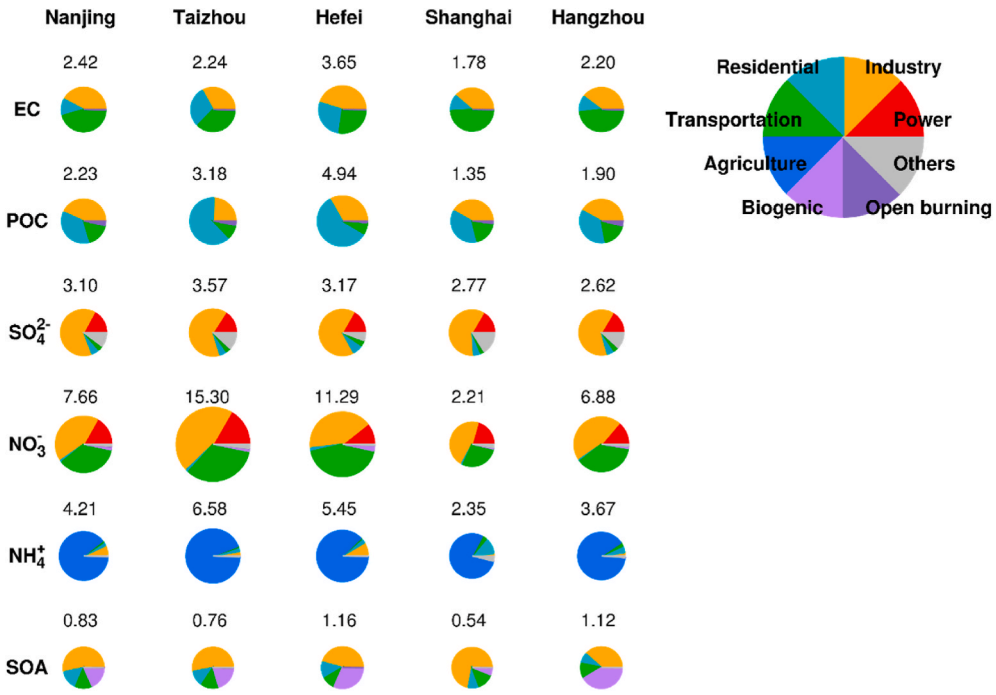

Fig. 8. Source contributions to $PM_{2.5}$ components. Units are $\mu g/m^3$.

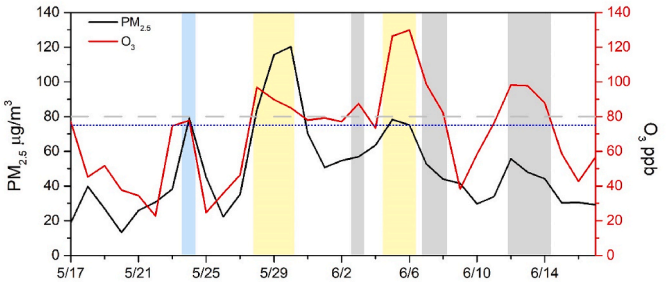

Fig. 9. Daily observed $PM_{2.5}$ and MDA8 O_3 concentrations at Taizhou during the EXPLORE-YRD campaign. The grey dash line is 80 ppbv for the National Ambient Air Quality Standard Grade II of O_3. The grey shadows cover the days of O_3-polluted. The blue dotted line is 75 $\mu g/m^3$ for the Grade II of daily average $PM_{2.5}$. The blue shadow represents $PM_{2.5}$ pollution day. The yellow shadows represent the period when occurred both O_3 and $PM_{2.5}$ pollution. (For interpretation of the references to color in this figure legend, the reader is referred to the Web version of this article.)

EC, and transportation is more important in SH, HZ, NJ and TZ, while the industrial sector is more important in HF with a contribution reaching 45%. POC, has concentrations ranging from 1.35 $\mu g/m^3$ in SH to 4.94 $\mu g/m^3$ in HF. In TZ and HF, residential emissions are the largest source of POC with contributions of 63% and 58.3% respectively, while the industrial sector is more important in NJ, HZ, and SH. For the secondary components, total concentrations of secondary inorganic aerosols dominate the total $PM_{2.5}$ mass concentrations. The industrial sector is the dominant source of SO2− 4 in all cities, followed by power generation. Industry, transportation, and power generation are the top three source contributors to NO− 3, and the source contribution pattern is similar in the five cities. Agriculture is the dominant source of NH+ 4, accounting for more than 75% of emissions in all cities. SOA are relatively low, and the sources of SOA vary among the five cities. In general, the industrial sector is the greatest source of SOA in NJ, TZ, HF, and SH, and biogenic emissions are the dominant source of SOA in HZ reaching more than 40%. In addition, residential emissions and transportation have contributions of 8.3–15% and 9.9–13.4% in the five cities, respectively.

3.3. Source contributions in different pollution episodes

Fig. 9 displays the time series of the observed $PM_{2.5}$ and O_3 concentrations during the entire episode. According to the National Ambient Air Quality Standard Grade II of O_3 and $PM_{2.5}$, in this study, we define EP1, EP2, and EP3 as only O_3-polluted, only $PM_{2.5}$-polluted, and

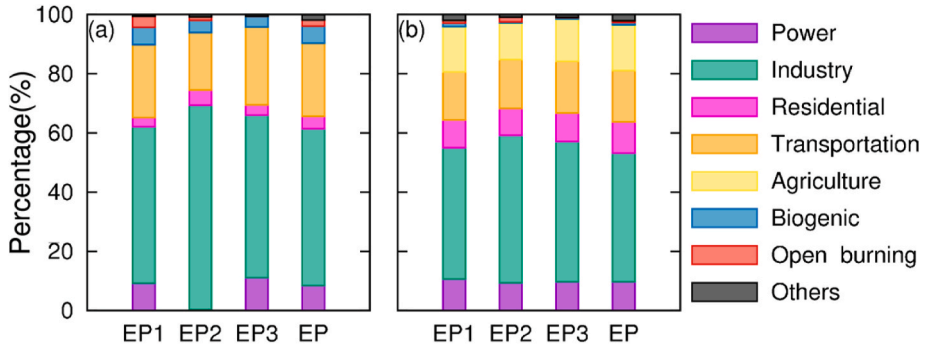

Fig. 10. Source contributions to (a) MDA8 O_3 and (b) 24-h $PM_{2.5}$ during different episodes at the TZ site. EP is denoted as the whole investigation period.

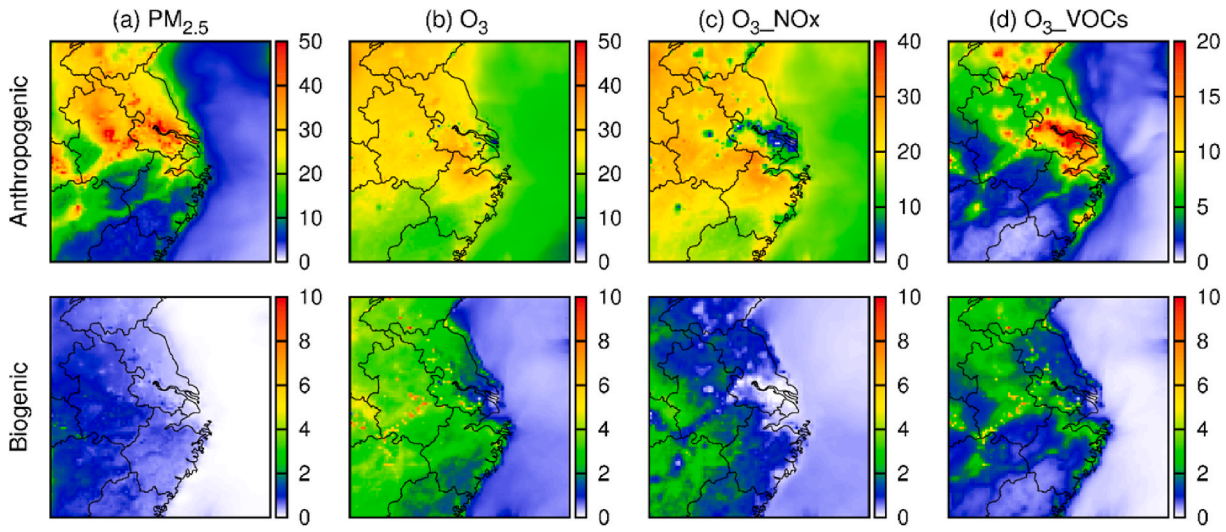

Fig. 11. Anthropogenic and biogenic source contributions to $PM_{2.5}$, O_3 and O_3 precursors. Units are μg/m^3 for $PM_{2.5}$ and ppb for O_3.

Table 4
Contributions of anthropogenic and natural sources to averaged $PM_{2.5}$, MDA8 O_3, O_3_NOx and O_3_VOCs concentrations in different cities.

		NJ	TZ	HF	SH	HZ
$PM_{2.5}$	Anthropogenic	99.1%	99.2%	98.5%	99.7%	97.9%
	Natural	0.9%	0.8%	1.5%	0.3%	2.1%
O_3	Anthropogenic	90.9%	94.1%	87.2%	98.1%	89.0%
	Natural	9.1%	5.9%	12.8%	1.9%	11.0%
O_3_NOx	Anthropogenic	95.7%	98.2%	95.4%	98.1%	98.3%
	Natural	4.3%	1.8%	4.6%	1.9%	1.7%
O_3_VOCs	Anthropogenic	89.8%	90.8%	81.9%	98.2%	82.1%
	Natural	10.2%	9.2%	18.1%	1.8%	17.9%

both O_3–$PM_{2.5}$-polluted days, respectively. EP1 occurred on 3, 7–8, and 12–14 June, with a maximum concentration of 100 ppb. EP2 occurred on 24 May, with a blue shadow. EP3 occurred on 28–30 May and 5–6 June. Fig. 10 shows the percentage of source contributions to MDA8 O_3 and 24-h $PM_{2.5}$ during different episodes at the TZ site and compares the source contributions to the average of the entire campaign period (denoted as 'EP'). The major sources are similar during different pollution episodes, with industry and transportation as the two main source sectors contributing to $PM_{2.5}$ and O_3. Minor differences can also be observed. O_3 contributed by the power sector significantly reduced to 0.3% during EP2. The contributions of biogenic sources and open burning to O_3 are 5.9% and 3.7%, respectively, in EP1, which is much greater than that in EP2 and EP3. This result suggests that biogenic sources and open burning contributions become more important on high O_3 days. In EP2, the contribution of the industrial sector to $PM_{2.5}$ increases, suggesting that controlling industrial emissions is especially necessary to reduce high $PM_{2.5}$ pollution events in the YRD region.

3.4. Comparison of anthropogenic and natural source contributions

Fig. 11 shows anthropogenic and biogenic source contributions to $PM_{2.5}$, O_3, and O_3 attributed to NOx and VOCs over the YRD region. Anthropogenic emissions are the dominant source contributing to $PM_{2.5}$, O_3, and O_3 attributed to NOx and VOCs. Areas of high anthropogenic source contributions to $PM_{2.5}$ are located in central and north Anhui Province and south Jiangsu Province. High O_3 concentrations contributed by anthropogenic sources mainly occur in the north and central YRD regions. The source contributions in the five cities are summarised in Table 4. During the study period, the biogenic source contributions to $PM_{2.5}$ are very small, with the largest contribution of 2.1% in the HZ. Biogenic contributions to O_3 are greater, reaching 12.8% in HF and 11.0% in HZ. Biogenic NOx is not important for O_3 formation in YRD, with contributions of 2–4%. Biogenic VOCs contribute 18% of O_3_VOCs in HF and HZ, but anthropogenic VOC emissions contribute the most O_3_VOCs in the five cities.

The accuracy of the predicted concentrations of O_3, $PM_{2.5}$, and its components and the predicted source contributions to these pollutants in this study are affected by a few factors, including uncertainties in emissions, inaccurate predictions of meteorological conditions, and imperfect model formulations of atmospheric physical and chemical processes. In general, the bias in the meteorology and imperfect model formulations affect O_3 and $PM_{2.5}$ formation from all sources. Although the absolute source contributions are biased, the relative contributions of different sources are less affected. Uncertainties in the emissions change both the absolute and relative contributions of different sources. Most uncertainties are associated with a few parameters used in emission calculation, including emission factors, activity levels, and emission control efficiency. The uncertainties of different parameters for different sources and pollutants vary significantly, resulting in substantial differences in the emission accuracy of different sources and pollutants (Huang et al., 2011; Zhao et al., 2011; Zheng et al., 2009). These uncertainties are carried into the air quality model simulations and affect the source apportionment results.

4. Conclusions

In this study, a source-oriented CMAQ model was applied to investigate the source apportionment of $PM_{2.5}$ and O_3 over the YRD region during the EXPLORE-YRD campaign. VOC sources play a more important role in O_3 formation than NOx sources in urban areas of the YRD, contributing 81.1%, 78.5%, 60.2%, and 55.1% to MDA8 O_3 in SH, NJ, HF, and HZ, respectively. However, in most areas over the YRD region, the concentration of O_3_NOx is higher than that of O_3_VOCs. The results indicate that O_3 formation is VOC-limited in the urban areas of the YRD and is NOx-limited in rural areas. Industry, transportation, and power sectors are the three main sources contributing to O_3_NOx. Industry, transportation, and biogenic emissions are the top three sources of O_3_VOCs. The industrial sector is also the largest source of $PM_{2.5}$ in the YRD region (contributing 9–25 μg/m^3), followed by transportation (2–7 μg/m^3) and agriculture (~6.5 μg/m^3). Industry, residential emissions, and transportation are the top three source sectors for primary $PM_{2.5}$. NO_3^- accounts for the largest fraction of $PM_{2.5}$, reaching 15.3 μg/m^3, and the major sources are industry, transportation, and power, similar to O_3_NOx. The industrial sector is also the largest source of SO_4^{2-} and an

important source of SOA, along with biogenic emissions. Industry and transportation are the two largest sources of O_3 and $PM_{2.5}$ in the YRD during most pollution episodes. The contribution of the industrial sector is the greatest during high $PM_{2.5}$ pollution episodes, and the contributions of biogenic sources and open burning are more important during high O_3 episodes. Overall, anthropogenic sources dominate the formation of O_3 and $PM_{2.5}$ pollution in the YRD, while biogenic emissions can contribute significantly to O_3_VOCs, accounting for 9–20% in the major urban areas of the YRD. The results suggest that it is necessary to reduce NOx and VOC emissions from the industry and transportation sectors in the YRD region to control O_3 and $PM_{2.5}$ pollution.

CRediT authorship contribution statement

Lin Li: Conceptualization, Data curation, Formal analysis, Writing - original draft. **Jianlin Hu:** Conceptualization, Funding acquisition, Methodology, Writing - review & editing. **Jingyi Li:** Funding acquisition, Methodology, Writing - review & editing. **Kangjia Gong:** Data curation, Formal analysis, Writing - review & editing. **Xueying Wang:** Data curation, Formal analysis, Writing - review & editing. **Qi Ying:** Methodology, Writing - review & editing. **Momei Qin:** Writing - review & editing. **Hong Liao:** Writing - review & editing. **Song Guo:** Writing - review & editing. **Min Hu:** Writing - review & editing. **Yuanhang Zhang:** Writing - review & editing.

Declaration of competing interest

The authors declare that they have no known competing financial interests or personal relationships that could have appeared to influence the work reported in this paper.

Acknowledgement

This work was supported by the National Key R&D Program of China (2018YFC0213800), the National Natural Science Foundation of China (41975162, 41675125 and 41705102), and Jiangsu Environmental Protection Research Project (2016015).

References

An, J., Zou, J., Wang, J., Lin, X., Zhu, B., 2015. Differences in ozone photochemical characteristics between the megacity Nanjing and its suburban surroundings, Yangtze River Delta, China. Environ. Sci. Pollut. Control Ser. 22, 19607–19617.
Fan, H., Zhao, C., Yang, Y., 2020. A comprehensive analysis of the spatio-temporal variation of urban air pollution in China during 2014–2018. Atmos. Environ. 220, 117066.
Feng, Z., Sun, J., Wan, W., Hu, E., Calatayud, V., 2014. Evidence of widespread ozone-induced visible injury on plants in Beijing, China. Environ. Pollut. 193, 296–301.
Gao, W., Tie, X., Xu, J., Huang, R., Mao, X., Zhou, G., Chang, L., 2017. Long-term trend of O3 in a mega City (Shanghai), China: characteristics, causes, and interactions with precursors. Sci. Total Environ. 603–604, 425–433.
Geng, F., Tie, X., Xu, J., Zhou, G., Peng, L., Gao, W., Tang, X., Zhao, C., 2008. Characterizations of ozone, NOx, and VOCs measured in Shanghai, China. Atmos. Environ. 42, 6873–6883.
Geng, F., Zhao, C., Tang, X., Lu, G., Tie, X., 2007. Analysis of ozone and VOCs measured in Shanghai: a case study. Atmos. Environ. 41, 989–1001.
Hu, J., Huang, L., Chen, M., Liao, H., Zhang, H., Wang, S., Zhang, Q., Ying, Q., 2017. Premature mortality attributable to particulate matter in China: source contributions and responses to reductions. Environ. Sci. Technol. 51 (17), 9950–9959.
Hu, J., Wu, L., Zheng, B., Zhang, Q., He, K., Chang, Q., Li, X., Yang, F., Ying, Q., Zhang, H., 2015. Source contributions and regional transport of primary particulate matter in China. Environ. Pollut. 207, 31–42.
Hua, Y., Cheng, Z., Wang, S., Jiang, J., Chen, D., Cai, S., Fu, X., Fu, Q., Chen, C., Xu, B., Yu, J., 2015. Characteristics and source apportionment of PM2.5 during a fall heavy haze episode in the Yangtze River Delta of China. Atmos. Environ. 123, 380–391.
Huang, C., Chen, C.H., Li, L., Cheng, Z., Wang, H.L., Huang, H.Y., Streets, D.G., Wang, Y. J., Zhang, G.F., Chen, Y.R., 2011. Emission inventory of anthropogenic air pollutants and VOC species in the Yangtze River Delta region, China. Atmos. Chem. Phys. 11, 4105–4120.
Lall, R., Kendall, M., Ito, K., Thurston, G.D., 2004. Estimation of historical annual PM2.5 exposures for health effects assessment. Atmos. Environ. 38, 5217–5226.
Li, L., An, J., Huang, L., Yan, R., Huang, C., Yarwood, G., 2019. Ozone source apportionment over the Yangtze River Delta region, China: investigation of regional transport, sectoral contributions and seasonal differences. Atmos. Environ. 202, 269–280.
Li, L., An, J.Y., Shi, Y.Y., Zhou, M., Yan, R.S., Huang, C., Wang, H.L., Lou, S.R., Wang, Q., Lu, Q., Wu, J., 2016. Source apportionment of surface ozone in the Yangtze River Delta, China in the summer of 2013. Atmos. Environ. 144, 194–207.
Li, L., An, J.Y., Zhou, M., Yan, R.S., Huang, C., Lu, Q., Lin, L., Wang, Y.J., Tao, S.K., Qiao, L.P., Zhu, S.H., Chen, C.H., 2015. Source apportionment of fine particles and its chemical components over the Yangtze River Delta, China during a heavy haze pollution episode. Atmos. Environ. 123, 415–429.
Li, L., Tan, Q., Zhang, Y., Feng, M., Qu, Y., An, J., Liu, X., 2017. Characteristics and source apportionment of PM2.5 during persistent extreme haze events in Chengdu, southwest China. Environmental pollution (Barking, Essex: 1987) 230, 718–729.
Liu, B., Song, N., Dai, Q., Mei, R., Sui, B., Bi, X., Feng, Y., 2016. Chemical composition and source apportionment of ambient PM2.5 during the non-heating period in Taian, China. Atmos. Res. 170, 23–33.
Liu, J., Shen, J., Cheng, Z., Wang, P., Ying, Q., Zhao, Q., Zhang, Y., Zhao, Y., Fu, Q., 2020. Source apportionment and regional transport of anthropogenic secondary organic aerosol during winter pollution periods in the Yangtze River Delta, China. Sci. Total Environ. 710, 135620.
Liu, T., Li, T.T., Zhang, Y.H., Xu, Y.J., Lao, X.Q., Rutherford, S., Chu, C., Luo, Y., Zhu, Q., Xu, X.J., Xie, H.Y., Liu, Z.R., Ma, W.J., 2013. The short-term effect of ambient ozone on mortality is modified by temperature in Guangzhou, China. Atmos. Environ. 76, 59–67.
Ma, Z., Xu, J., Quan, W., Zhang, Z., Lin, W., Xu, X., 2016. Significant increase of surface ozone at a rural site, north of eastern China. Atmos. Chem. Phys. 16, 3969–3977.
Menon, S., Unger, N., Koch, D., Francis, J., Garrett, T., Sednev, I., Shindell, D., Streets, D., 2008. Aerosol climate effects and air quality impacts from 1980 to 2030. Environ. Res. Lett. 3, 024004.
Ou, J., Yuan, Z., Zheng, J., Huang, Z., Shao, M., Li, Z., Huang, X., Guo, H., Louie, P.K.K., 2016. Ambient ozone control in a photochemically active region: short-term despiking or long-term attainment? Environ. Sci. Technol. 50, 5720–5728.
Qiao, X., Xiao, W., Jaffe, D., Kota, S.H., Ying, Q., Tang, Y., 2015. Atmospheric wet deposition of sulfur and nitrogen in Jiuzhaigou national nature reserve, Sichuan province, China. Sci. Total Environ. 511, 28–36.
Qiao, X., Ying, Q., Li, X., Zhang, H., Hu, J., Tang, Y., Chen, X., 2018. Source apportionment of PM2.5 for 25 Chinese provincial capitals and municipalities using a source-oriented Community Multiscale Air Quality model. Sci. Total Environ. 612, 462–471.
Shi, Z., Li, J., Huang, L., Wang, P., Wu, L., Ying, Q., Zhang, H., Lu, L., Liu, X., Liao, H., Hu, J., 2017. Source apportionment of fine particulate matter in China in 2013 using a source-oriented chemical transport model. Sci. Total Environ. 601–602, 1476–1487.
Shu, L., Wang, T., Han, H., Xie, M., Chen, P., Li, M., Wu, H., 2020. Summertime ozone pollution in the Yangtze River Delta of eastern China during 2013–2017: synoptic impacts and source apportionment. Environ. Pollut. 257, 113631.
Timmermans, R., Kranenburg, R., Manders, A., Hendriks, C., Segers, A., Dammers, E., Zhang, Q., Wang, L., Liu, Z., Zeng, L., Denier van der Gon, H., Schaap, M., 2017. Source apportionment of PM2.5 across China using LOTOS-EUROS. Atmos. Environ. 164, 370–386.
Wang, L., Wei, Z., Wei, W., Fu, J.S., Meng, C., Ma, S., 2015. Source apportionment of PM2.5 in top polluted cities in Hebei, China using the CMAQ model. Atmos. Environ. 122, 723–736.
Wang, N., Lyu, X., Deng, X., Guo, H., Deng, T., Li, Y., Changqin, Y., Li, F., Wang, S.Q., 2016. Assessment of regional air quality resulting from emission control in the Pearl River Delta region, southern China. The Science of the Total Environment 573.
Wang, P., Chen, Y., Hu, J., Zhang, H., Ying, Q., 2019a. Attribution of tropospheric ozone to NOx and VOC emissions: considering ozone formation in the transition regime. Environ. Sci. Technol. 53, 1404–1412.
Wang, P., Chen, Y., Hu, J., Zhang, H., Ying, Q., 2019b. Source apportionment of summertime ozone in China using a source-oriented chemical transport model. Atmos. Environ. 211, 79–90.
Wang, P., Ying, Q., Zhang, H., Hu, J., Lin, Y., Mao, H., 2018. Source apportionment of secondary organic aerosol in China using a regional source-oriented chemical transport model and two emission inventories. Environ. Pollut. 237, 756–766.
Wang, X., Li, L., Gong, K., Mao, J., Li, J., Liu, Z., Liao, H., Qiu, W., Yu, Y., Dong, H., Guo, S., Hu, M., Zeng, L., Zhang, Y., 2020. Modeling Air Quality during the EXPLORE-YRD Campaign - Part I. Model Performance Evaluation and Impacts of Meteorological Inputs and Grid Resolutions. Atmospheric Environment (submitted for publication).
Wang, Y., Wang, H., Guo, H., Lyu, X., Cheng, H., Ling, Z., Louie, P.K.K., Simpson, I.J., Meinardi, S., Blake, D.R., 2017. Long-term O3–precursor relationships in Hong Kong: field observation and model simulation. Atmos. Chem. Phys. 17, 10919–10935.
Wu, S.-P., Schwab, J., Yang, B.-Y., Zheng, A., Yuan, C.-S., 2015. Two-years PM2.5 observations at four urban sites along the coast of southeastern China. Aerosol Air Qual. Res. 15, 1799–1812.
Yang, F., Tan, J., Zhao, Q., Du, Z., He, K., Ma, Y., Duan, F., Chen, G., Zhao, Q., 2011. Characteristics of PM2.5 speciation in representative megacities and across China. Atmos. Chem. Phys. 11, 5207–5219.
Ying, Q., Feng, M., Song, D., Wu, L., Hu, J., Zhang, H., Kleeman, M.J., Li, X., 2018. Improve regional distribution and source apportionment of PM2.5 trace elements in China using inventory-observation constrained emission factors. Sci. Total Environ. 624, 355–365.
Zhang, H., Hu, J., Kleeman, M., Ying, Q., 2014. Source apportionment of sulfate and nitrate particulate matter in the Eastern United States and effectiveness of emission control programs. Sci. Total Environ. 490, 171–181.

Zhang, H., Ying, Q., 2011a. Contributions of local and regional sources of NOx to ozone concentrations in Southeast Texas. Atmos. Environ. 45, 2877–2887.
Zhang, H., Ying, Q., 2011b. Secondary organic aerosol formation and source apportionment in Southeast Texas. Atmos. Environ. 45, 3217–3227.
Zhang, Z., Zhang, X., Gong, D., Quan, W., Zhao, X., Ma, Z., Kim, S.-J., 2015. Evolution of surface O3 and PM2.5 concentrations and their relationships with meteorological conditions over the last decade in Beijing. Atmos. Environ. 108, 67–75.
Zhao, Y., Nielsen, C.P., Lei, Y., McElroy, M.B., Hao, J., 2011. Quantifying the uncertainties of a bottom-up emission inventory of anthropogenic atmospheric pollutants in China. Atmos. Chem. Phys. 11, 2295–2308.
Zheng, J., Zhang, L., Che, W., Zheng, Z., Yin, S., 2009. A highly resolved temporal and spatial air pollutant emission inventory for the Pearl River Delta region, China and its uncertainty assessment. Atmos. Environ. 43, 5112–5122.